

Quantum Multiplier Based on Exponent Adder

Junpeng Zhan¹

¹Alfred University, Alfred, NY 14802, United States

(Dated: September 19, 2023)

Abstract

Quantum multiplication is a fundamental operation in quantum computing. Most existing quantum multipliers require $O(n)$ qubits to multiply two n -bit integer numbers, limiting their applicability to multiply large integer numbers using near-term quantum computers. This paper proposes a new approach, the Quantum Multiplier Based on Exponent Adder (QMbead), which addresses this issue by requiring only $\log_2(n)$ qubits to multiply two n -bit integer numbers. QMbead uses a so-called exponent encoding to represent the two multiplicands as two superposition states, respectively, and then employs a quantum adder to obtain the sum of these two superposition states, and subsequently measures the outputs of the quantum adder to calculate the product of the multiplicands. The paper presents two types of quantum adders based on the quantum Fourier transform (QFT) for use in QMbead. The circuit depth of QMbead is determined by the chosen quantum adder, being $O(\log_2^2 n)$ when using the two QFT-based adders. The multiplicand can be either an integer or a decimal number. QMbead has been implemented on quantum simulators to compute products with a bit length of up to 273 bits using only 17 qubits. This establishes QMbead as an efficient solution for multiplying large integer or decimal numbers with many bits.

I. Introduction

Quantum computing, with its potential for exponential speedup in solving complex problems, has revolutionized the landscape of computational algorithms. In the domain of quantum computing, the pursuit for highly efficient quantum arithmetic algorithms is of paramount importance. Shor's algorithm [1], [2] demonstrated an exponential advantage of quantum computing in factoring large numbers, a problem crucial to cryptography. This breakthrough has motivated extensive research and development efforts aimed at advancing quantum arithmetic, including, but not limited to, adders [3]–[6], modular adder [5]–[8], multipliers [6], [9]–[14], modular multiplication [8], [9], [15], matrix multiplication [16]–[20], and modular exponentiation [5], [8], [21].

This paper focuses on quantum multipliers. A common and straightforward approach to construct a quantum multiplier is through the repetitive utilization of controlled quantum adders, wherein the result is accumulated within a dedicated register [9]. Many quantum multipliers [6], [9] belong to this approach. An alternative approach is based on Quantum Fourier Transform (QFT) and, typically, comprises a QFT, controlled phase rotation gates, and an inverse QFT [10]. The multiplier using this approach does not require ancillary qubits but could have a high circuit depth. Furthermore, there exist other types of quantum multipliers as discussed below. Paper [11] introduces a quantum Karatsuba multiplication, which uses about 10 qubits per bit of input data. Paper [22] proposes a Repeat-Until-Success circuit, which encodes integer numbers as rotation angles within the amplitudes of qubits, subsequently multiplies these rotation angles, and outputs the product as a rotation angle. A common feature shared by these approaches, except for [22], is that they all encode an integer number in binary number system within the computational basis, which requires n qubits to represent an n -bit number, where each bit is either 0 or 1.

In this paper, we introduce a new quantum multiplier, called Quantum Multiplier Based on Exponent Adder (QMbead), which uses a new encoding method, called *exponent encoding*. This method represents an integer as a superposition of exponents obtained from its expression as a sum of distinct powers of 2, composing the integer. For example, the integer 14 can be represented as a superposition of $|11\rangle$, $|10\rangle$, and $|01\rangle$, respectively corresponding to the three exponents in this expression: $14 = 2^3 + 2^2 + 2^1$. QMbead takes two integer numbers as input, each employing exponent encoding, and summates them using a

quantum adder. The addition results are then measured to derive the product of the two integer numbers. QMbead’s key advantage lies in its ability to represent an n -bit number using only $\log_2 n$ qubits. Consequently, QMbead can use $2 \log_2 n + 1$ qubits, without requiring any ancillary qubits, to multiply two n -bit numbers. This qubit requirement is *exponentially lower* compared to the common multipliers mentioned in the previous paragraph. Furthermore, QMbead has low circuit depth, equal to that of a quantum adder used for adding two $\log_2 n$ -bit numbers. With its efficient use of qubits and low circuit depth, QMbead can multiply exceptionally large integer numbers. Here, we exemplify the advantage of QMbead: when tasked with multiplying two 1024-bit numbers, QMbead needs only 21 qubits, while a QFT-based multiplier requires 3073 qubits. Note that throughout the paper, when we mention the bit length of an integer, we specifically refer to its bit length when expressed in binary form. For instance, the bit length of 14 is 4, corresponding to its binary form of 1110.

The remainder of the paper is organized as follows. Section II details the QMbead method. Section III conducts a complexity analysis of the QMbead method. Additionally, Section IV presents the numerical results obtained by employing QMbead to multiply both integer and decimal numbers. Finally, in Section V, we draw our conclusions.

II. Method

In this section, we start with three warm up examples to illustrate the main idea of the QMbead method. Then, we detail the method and provide its Pseudo code. Lastly, we conduct an analysis of the method’s complexity.

Warm up examples

In this subsection, we present three illustrative examples of multiplying two numbers. These examples aim to elucidate the motivation and fundamental concept behind the QMbead method.

Example 1: multiply two integers, 3 and 5,

$$\begin{aligned}
 u \times v &= 3 \times 5 = (2^1 + 2^0) \times (2^2 + 2^0) \\
 &= 2^1 \times (2^2 + 2^0) + 2^0 \times (2^2 + 2^0) \\
 &= (2^{1+2} + 2^{1+0}) + (2^{0+2} + 2^{0+0}) \\
 &= 2^3 + 2^1 + 2^2 + 2^0 = 15
 \end{aligned} \tag{1}$$

Example 2: multiply two integers, 6 and 7,

$$\begin{aligned}
 u \times v &= 6 \times 7 = (2^2 + 2^1) \times (2^2 + 2^1 + 2^0) \\
 &= 2^2 \times (2^2 + 2^1 + 2^0) + 2^1 \times (2^2 + 2^1 + 2^0) \\
 &= (2^{2+2} + 2^{2+1} + 2^{2+0}) + (2^{1+2} + 2^{1+1} + 2^{1+0}) \\
 &= 2^4 + 2^3 + 2^2 + 2^3 + 2^2 + 2^1 = 42
 \end{aligned} \tag{2}$$

These two examples show that we can multiply two integers (in decimal system) by initially decomposing each integer into a sum of distinct powers of 2. Subsequently, applying the distributive property of multiplication, we add the corresponding exponents to obtain the final product expressed in a sum of powers of 2.

As we delve into the QMbead method, we’ll introduce a unique approach to multiply decimal numbers. Here is an example.

Example 3: multiply two decimal numbers, 2.5 and 1.75,

$$\begin{aligned}
 u \times v &= 2.5 \times 1.75 = (2^1 + 2^{-1}) \times (2^0 + 2^{-1} + 2^{-2}) \\
 &= 2^{-1} \times (2^2 + 2^0) \times 2^{-2} \times (2^2 + 2^1 + 2^0) \\
 &= 2^{-3} \times (2^2 + 2^0) \times (2^2 + 2^1 + 2^0) \\
 &= 2^{-3} \times [(2^2) \times (2^2 + 2^1 + 2^0) + (2^0) \times (2^2 + 2^1 + 2^0)]
 \end{aligned}$$

$$\begin{aligned}
&= 2^{-3} \times [(2^{2+2} + 2^{2+1} + 2^{2+0}) + (2^{0+2} + 2^{0+1} + 2^{0+0})] \\
&= 2^{-3} \times [2^4 + 2^3 + 2^2 + 2^2 + 2^1 + 2^0] = 2^{-3} \times 35 = 4.375
\end{aligned} \tag{3}$$

Example 3 shows that we can convert a decimal number into the sum of distinct powers of 2, where the exponent can be positive or negative. Then, we multiply each decimal number by a coefficient such that the exponents become non-negative. Then the rest of the process is the same as Examples 1 and 2. In other words, we convert the decimal numbers into integer numbers with appropriate coefficients, followed by multiplying these integer numbers.

High-level idea of QMbead: At the core of the QMbead method lies adding the exponents together. We use a quantum adder to implement the addition, leveraging the power of superposition, as elaborated below. Given that each of the number, u and v , corresponds to one or more exponents, and the multiplication involves adding each exponent from u to each exponent from v , quantum adder is the ideal tool for this task. To facilitate this process, we employ two quantum states: $|\psi\rangle$ to represent a superposition of all exponents from u and $|\phi\rangle$ to represent a superposition of all exponents from v . A quantum adder can add $|\psi\rangle$ and $|\phi\rangle$ together, where $|\psi\rangle$ and $|\phi\rangle$ can each be either a pure state or a mixed state. In Example 1, u has exponents 1 and 0, which can be represented by $|\psi\rangle$, i.e., $|\psi\rangle = (|1\rangle + |0\rangle)/\sqrt{2}$. Similarly, v has exponents 2 and 0, which can be represented by $|\phi\rangle$, i.e., $|\phi\rangle = (|10\rangle + |00\rangle)/\sqrt{2}$. Our objective in employing the quantum adder is to obtain the desired output: $(|11\rangle + |01\rangle + |10\rangle + |00\rangle)/2$, which is obtained by adding each element in $|\psi\rangle$ with each element in $|\phi\rangle$.

QMbead Method

In this subsection, we detail the QMbead method, along with its Pseudo code.

First, we transform u into a binary representation denoted as $b_{n_u-1}b_{n_u-2} \cdots b_2b_1b_0$, which is then converted into a weighted sum of 2^α , as shown in Eq. (4).

$$u = b_{n_u-1}b_{n_u-2} \cdots b_2b_1b_0 = \sum_{\alpha=0}^{n_u-1} b_\alpha 2^\alpha \tag{4}$$

where $b_\alpha \in \{0,1\}$.

Similarly, we transform v into a binary representation denoted as $b_{n_v-1}b_{n_v-2} \cdots b_2b_1b_0$, which is then converted into a weighted sum of 2^β , as shown in Eq. (5).

$$v = b_{n_v-1}b_{n_v-2} \cdots b_2b_1b_0 = \sum_{\beta=0}^{n_v-1} b_\beta 2^\beta \tag{5}$$

where $b_\beta \in \{0,1\}$.

Then, let $|\psi\rangle$ represent the superposition of all exponents associated with u , as expressed in Eq. (6).

$$|\psi\rangle = \left(1/\sqrt{\sum_{\alpha=0}^{n_u-1} b_\alpha^2}\right) \sum_{\alpha=0}^{n_u-1} b_\alpha |\alpha\rangle \tag{6}$$

Similarly, let $|\phi\rangle$ represent the superposition of all exponents associated with v , as expressed in Eq. (7).

$$|\phi\rangle = \left(1/\sqrt{\sum_{\beta=0}^{n_v-1} b_\beta^2}\right) \sum_{\beta=0}^{n_v-1} b_\beta |\beta\rangle \tag{7}$$

Then, we use a quantum adder to add states $|\psi\rangle$ and $|\phi\rangle$, with their sum being represented as the output state of the quantum adder, as described in Eq. (8) or Eq. (9). The details of quantum adder are given in the next subsection.

$$|\psi + \phi\rangle = \left(1/\sqrt{\sum_{\alpha=0}^{n_u-1} \sum_{\beta=0}^{n_v-1} b_\alpha^2 b_\beta^2}\right) \sum_{\alpha=0}^{n_u-1} \sum_{\beta=0}^{n_v-1} b_\alpha b_\beta |\alpha + \beta\rangle \tag{8}$$

We can reformulate Eq. (8) as

$$|\psi + \phi\rangle = \left(1/\sqrt{\sum_{\gamma=0}^{n_u+n_v-2} c_\gamma^2}\right) \sum_{\gamma=0}^{n_u+n_v-2} c_\gamma |\gamma\rangle \tag{9}$$

By measuring the output of the quantum adder, i.e., state $|\psi + \phi\rangle$, we obtain state $|\gamma\rangle$ with a probability of p_γ . If only one state, denoted as $|\gamma\rangle$, is measured, we obtain the *product* as

$$u \times v = 2^\gamma \quad (10)$$

On the other hand, if multiple states are measured, denoted as $|\gamma_0\rangle, |\gamma_1\rangle, \dots, |\gamma_{n_\gamma}\rangle$, with the probabilities of $p_0, p_1, \dots, p_{n_\gamma}$, respectively, then we can obtain the *product* as

$$u \times v = \sum_{i=0}^{n_\gamma} (p_i/p_{\min}) 2^{\gamma_i} \quad (11)$$

where p_{\min} represents the minimum value among all probabilities $p_1, p_2, \dots, p_{n_\gamma}$, and γ_i is converted into its decimal form.

Here we discuss how to set the number of shots required to estimate the p_i and p_{\min} in Eq. (11). In quantum computing, we perform measurements multiple times, referred to as "*shots*", to observe each possible output and estimate its probability based on the frequency of measurement occurrences. To simplify expression, we refer to γ_i as the *exponent of the product*. The number of exponents of the product with non-zero probability (p_i) affects the number of shots required to measure both low-probability and high-probability exponents of the product. However, the number of exponents with non-zero probability is unknown until we determine the product value, although we can set it as the product of the number of b_α that is equal to 1 and the number of b_β that is equal to 1. Alternatively, we can set the number of shots based on the number of qubits needed to represent the product. Since we need to round each p_i/p_{\min} in Eq. (11) to the nearest integer and measurement outcomes are probabilistic, a sufficiently large number of shots is essential to accurately calculate p_i/p_{\min} . We can set the number of shots to be $C_0 \times 2^{1+\lceil \log_2 n_m \rceil}$ such that we will obtain the lowest-probability exponent of product around C_0 times, where C_0 denotes a coefficient (we can choose C_0 within the range of 1000~10000), $1 + \lceil \log_2 n_m \rceil$ represents the number of qubits required to represent the exponents of the product, and n_m is the larger of the bit lengths of the two multiplicands, i.e., $n_m = \max(n_u, n_v)$.

To provide an intuitive understanding of how the number of shots needed scales with the bit length n_m , we plot the function $2000 \times 2^{1+\lceil \log_2 n_m \rceil}$ in Fig. S1. The figure shows a piecewise linear growth in the number of shots with respect to the bit length of the larger multiplicand.

The Pseudo code for QMbead is given in Algorithm 1.

Algorithm 1: Pseudo code for QMbead

Input: integer numbers u and v .

Output: the product of the two numbers, denoted as $u \times v$.

- 1 Convert u into a sum of distinct powers of 2 using Eq. (4) and v into a similar representation using Eq. (5).
 - 2 Obtain states $|\psi\rangle$ and $|\phi\rangle$, each representing a superposition of their respective exponents, using Eqs. (6) and (7), respectively.
 - 3 Utilize a quantum adder to add states $|\psi\rangle$ and $|\phi\rangle$, resulting in the output state $|\psi + \phi\rangle$, as described in Eq. (9).
 - 4 Measure the output state of the quantum adder, i.e., $|\psi + \phi\rangle$, to calculate the product of u and v . If only one state is measured, the product is determined by Eq. (10). If multiple states are measured, the product is computed using Eq. (11).
-

Quantum Adder

Here we provide two versions of QFT-based quantum adders to complete step 3 in Algorithm 1. The first version is an in-place quantum adder, as shown in Fig. 1. The input and output of this circuit can be written as $|\phi\rangle_B|0\rangle_C|\psi\rangle_A$ and $|\phi\rangle_B|\phi + \psi\rangle_{CA}$.

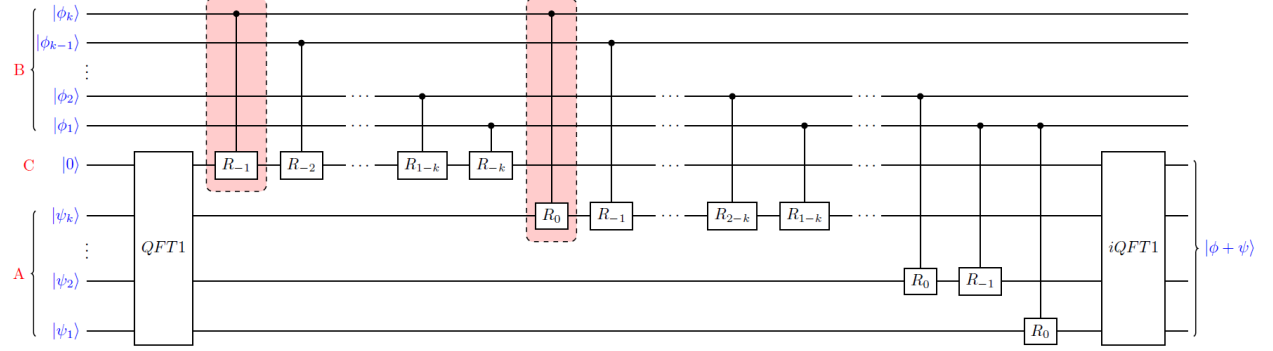


Fig. 1. The in-place quantum adder based on QFT (version 1). It takes states $|\phi\rangle$ and $|\psi\rangle$ as input and outputs their sum $|\phi + \psi\rangle$. It consists of three registers, B, C, and A (indicated by the red letters on the leftmost side). Register C contains only one qubit, called *carry qubit*. Register A comprises k qubits, used for representing state $|\psi\rangle$. Register B is for state $|\phi\rangle$ and has k qubits, although it can have fewer qubits if needed. For example, if $|\phi\rangle$ has only $k-1$ qubits, then the top wire, $|\phi_k\rangle$, and the two controlled rotation gates in dashed red box can be deleted. The ‘ $QFT1$ ’ and ‘ $iQFT1$ ’ denote the QFT without swap gates and its inverse, respectively.

In both Figs. 1 and 2, the symbol R_x represents the gate $\begin{bmatrix} 1 & 0 \\ 0 & e^{i\pi 2^x} \end{bmatrix}$. Note that $R_z(\theta) = e^{-i\theta/2} \begin{bmatrix} 1 & 0 \\ 0 & e^{i\theta} \end{bmatrix}$. Then we can realize the R_x gate as an $R_z(\theta)$ gate with $\theta = \pi 2^x$, up to a global phase difference.

Note that the carry qubit (with the red ‘C’ on the leftmost side) in the circuit given in Fig. 1 does not have a controlled R_0 gate, while all the k wires for state $|\psi\rangle$ has a controlled R_0 gate. Here state $|\phi\rangle$ remains unchanged (i.e., the input and output of register B are the same), while state $|\psi\rangle$ can change during the operation of this circuit. This quantum adder is like, but slightly different from, the one in [23]. Importantly, the circuit in Fig. 1 does not suffer from overflow issues, unlike the latter, and it allows the number of qubits in register B to be equal to or less than that in register A.

If we need to maintain both the states $|\phi\rangle$ and $|\psi\rangle$ unchanged throughout the computation, we can use the out-of-place quantum adder depicted in Fig. 2, where $|s_i\rangle = |0\rangle$ for all i in $[1, k+1]$. The input and output of this circuit can be written as $|\phi\rangle|\psi\rangle|0\rangle$ and $|\phi\rangle|\psi\rangle|\psi + \phi\rangle$, respectively. This adder requires more qubits and has a higher circuit depth compared to the one shown in Fig. 1.

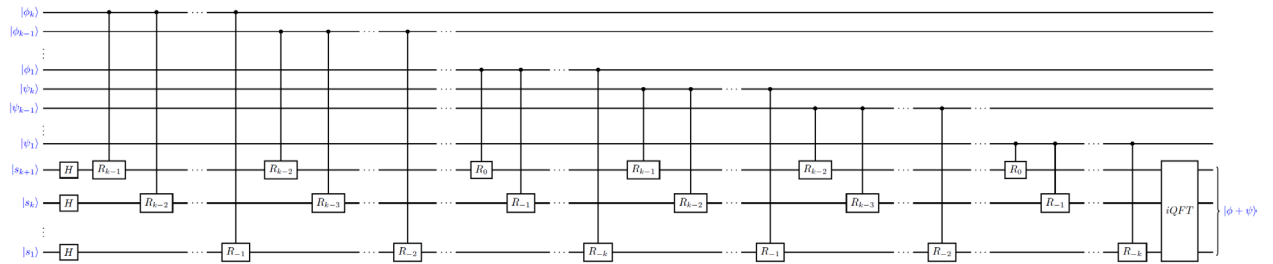


Fig. 2. The out-of-place quantum adder based on QFT (version 2). It takes states $|\phi\rangle$ and $|\psi\rangle$ as input and produces their sum $|\phi + \psi\rangle$ as output. This adder ensures that the states $|\phi\rangle$ and $|\psi\rangle$ remain unchanged throughout the computation.

III. Complexity Analysis

In this section, we provide the complexity analysis, including the number of qubits and the circuit depth, for the QMbead using two versions of adders, as shown in Figs. 1 and 2, respectively.

As shown in Eq. (4), integer u consists of n_u binary bits and it is expressed as a superposition of states $|\alpha\rangle$ according to Eq. (6). The maximum value of α is $n_u - 1$, which can be represented by $\lceil \log_2 n_u \rceil$ qubits, where the notation $\lceil x \rceil$ denotes the smallest integer greater than or equal to x . Similarly, we use $\lceil \log_2 n_v \rceil$ qubits to represent the components associated with the integer v . For instance, we can

- represent a 9-bit number, 384 (equal to $2^8 + 2^7$), as a four-qubit state: $(|1000\rangle + |0111\rangle)/\sqrt{2}$,
- represent a 21-bit number, 1835008 (equal to $2^{20} + 2^{19} + 2^{18}$), as a 5-qubit state: $(|10100\rangle + |10011\rangle + |10010\rangle)/\sqrt{3}$, and
- represent a 1024-bit number, $2^{1023} + 2^{1022}$ (approximating to 1.35×10^{308}), as a 10-qubit state $(|1\ 111\ 111\ 111\rangle + |1\ 111\ 111\ 110\rangle)/\sqrt{2}$.

For simplicity, we assume $n_u = n_v = n$ in the rest of the paper, meaning integers u and v , when expressed in binary form, have an equal number of binary bits. However, it is worth noting that the circuits shown in Figs. 1 and 2 can handle two integers with different bit lengths, represented by different numbers of qubits.

For the QMbead using the quantum adder in Fig. 1, it needs $2\lceil \log_2 n \rceil + 1$ qubits for multiplying integers u and v . In the case of the QMbead utilizing the quantum adder given in Fig. 2, it needs $3\lceil \log_2 n \rceil + 1$ qubits for multiplying integers u and v . Note that in the following three paragraphs, $k = \lceil \log_2 n \rceil$.

In Fig. 1, the $(k+1)$ -qubit QFT without swap gates and its inverse each has a circuit depth of $(k+2)(k+1)/2$ and the depth of the controlled rotation gates is $(k+3)k/2$. If we consider controlled rotation gates on different qubits can be applied in parallel [23], the depth of controlled rotation gates is k . Then we can express the total depth of the circuit given in Fig. 1 as $k + 2 \times (k+2)(k+1)/2 = k^2 + 4k + 2$.

Now we consider Fig. 2. The circuit depth of the Hadamard gates is 1. The inverse of the $(k+1)$ -qubit QFT, denoted as $iQFT$, has a circuit depth of $\frac{(k+2)(k+1)}{2} + \lfloor \frac{k+1}{2} \rfloor$, where the notation $\lfloor x \rfloor$ denotes the largest integer smaller than or equal to x . The depth of controlled rotation gates is $2k(k+1)$. If we consider controlled rotation gates on different qubits can be applied in parallel, the depth of the $iQFT$ reduces to $(k+2)(k+1)/2 + 1$ and the depth of controlled rotation gates becomes $2(k+1)$. Then we can express the total depth of the circuit given in Fig. 2 as $1 + (k+2)(k+1)/2 + 1 + 2(k+1) = (k^2 + 7k)/2 + 4$.

For the ease of comparison, Table I summarizes the number of qubits and the circuit depth of the QMbead, where ‘v1’ represents the version 1 circuit in Fig. 1 and ‘v2’ represents the version 2 circuit in Fig. 2.

It is important to highlight that in the previous subsection, we demonstrated two quantum adders based on QFT. However, there are alternative types of quantum adders, like the logarithmic-depth quantum carry lookahead adder discussed in [4], which can be implemented in QMbead to further reduce the circuit depth.

Table I. Qubit count and circuit depth for QMbead using quantum adders from Figs. 1 and 2.

	# of qubits	Circuit depth*
QMbead (v1)	$2\lceil \log_2 n \rceil + 1$	$\lceil \log_2 n \rceil^2 + 4\lceil \log_2 n \rceil + 2$
QMbead (v2)	$3\lceil \log_2 n \rceil + 1$	$(\lceil \log_2 n \rceil^2 + 7\lceil \log_2 n \rceil)/2 + 4$

* Parallel application of controlled rotation gates is considered for circuit depth calculation. We assume $n_u = n_v = n$.

IV. Numerical Results

To verify its effectiveness, we executed the QMbead on PennyLane's qubit device [24], performing multiplications for 13 pairs of integer numbers and 3 pairs of decimal numbers. The obtained results are presented

in Table II. We successfully obtained the correct product result for each pair of u and v listed in Table II using a single run of the quantum circuit presented in Fig. 1 with the number of shots as specified in the table. It is worth noting that even though we utilized many shots in measurement, the theoretical output of the circuit is deterministic. In other words, measuring the output will yield the correct product with a 100% certainty.

Table II shows that as the bit length of the product increases from 4 to 273, the number of qubits used by QMbead, utilizing the quantum adder from Fig. 1, grows slowly. We plot their relationship in Fig. 3, showcasing a logarithmic correlation, i.e., the number of qubits required by QMbead is the logarithm of the bit length of the product.

Table II. The multiplicands, u and v , and the product obtained by QMbead with the quantum adder given in Fig. 1. The number of shots, the bit length of the product, and the total number of qubits used in the QMbead are provided in the last three columns.

id	Multiplicand u	Multiplicand v	Product ($u \times v$)	# of shots	Bit length of product	# of qubits
1	3	5	15	1×10^5	4	4
2	33	100	3300	1×10^5	12	7
3	2345	5678	13314910	1×10^5	24	9
4	234501	567801	133149902301	1×10^5	37	11
5	23450101	56780101	1331499103240201	1×10^6	51	11
6	2345010101	5678010101	13314991040425030201	1×10^6	64	12
7	8978923748987	8984957438475849	80675247727968202502337714963	5×10^6	97	13
8	24587098456973459873	93847898723487384738	2307447525894458211799840656192155618274	5×10^7	131	15
9	98734587398457983758948	87234593847548978394754	8613071630409809722603055112891858675923758792	5×10^7	153	15
10	87349853987589789837437878	94543085490894758478947548	8258324713165875922142248753007708733319714270423144	5×10^7	173	15
11	98734574983957438978459843787	91398475934873485748398475397	9024189675611195666675703027302141983724295908377582808439	1×10^8	193	15
12	87892734987329734982798374239878729	99787498783927389473829348739287348	8770596185664218247269027408953463166804991960126150471650153404020692	1×10^8	233	15
13	98789236479326873476287376473627847267623	92934837483278492837489283478928374829373	9180961637303410170533798160931075913254844659074625888400424445374174806892290379	1×10^8	273	17
14	0.567	0.0004	0.0002268	1×10^5	12*	7
15	2.5	1.75	4.375	1×10^5	13*	7
16	136872.345502	2343651.74543455	320781111437.483078727894100	5×10^6	89*	13

*The bit lengths in these three rows correspond to the bit length of the scaled product, which is an integer.

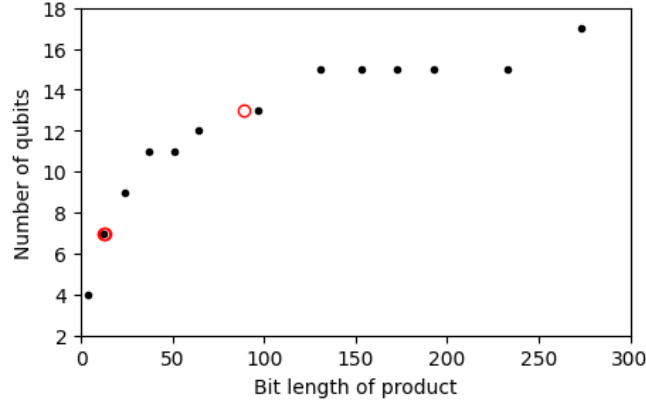


Fig. 3. Scatter plot of the relationship between the number of qubits used by QMbead with the quantum adder given in Fig. 1 and the bit length of the product. The black dots correspond to the integer cases (the first 13 cases in Table II), while the red circles represent the decimal cases (the last 3 cases in Table II).

Here we present the measurement results for three cases: 3×5 , 33×100 , and 2345×5678 , shown as bar plots in Figs. 4-6, respectively. The left panel of each figure (Figs. 4-6) provides the number of counts for each measured state, denoted by the digits at the bottom of each bar. The right panel of each of figure (Figs. 4-6) shows the coefficient p_i/p_{\min} in Eq. (11). These coefficients have been rounded to the nearest integer for each exponent of the product, i.e., γ_i in Eq. (11), where the exponent of the product is represented by the digits in binary form at the bottom of each bar. Note that both panels share the same x-axis labels, despite their distinct meanings. The former indicates measured states, while the latter represents exponents. Each measured state is associated with a specific exponent. For instance, the x-axis labels of the four bars in Fig. 4 are 000, 001, 010, and 011, representing the states $|000\rangle$, $|001\rangle$, $|010\rangle$, $|011\rangle$, and the corresponding exponents in binary form, respectively.

We calculate the probability p_i in Eq. (11) by dividing the number of counts by the total number of shots. We illustrate how to derive the correct product from the right panel of each figure (Figs. 4-6), as detailed in each figure caption, where the exponents in binary form are converted to decimal form.

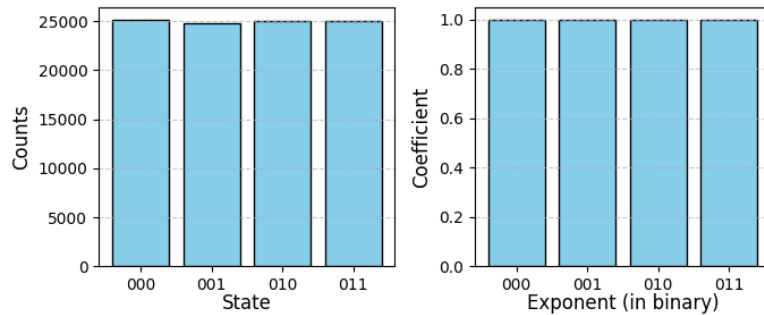


Fig. 4. The measurement counts (left panel) and the rounded coefficient p_i/p_{\min} in Eq. (11) (right panel) obtained from the output of QMbead for calculating 3×5 . According to Eq. (11), the product is determined from the right panel as $1 \times 2^0 + 1 \times 2^1 + 1 \times 2^2 + 1 \times 2^3$, which is equal to 15, where the exponents are obtained by converting the binary digits to their respective decimal values.

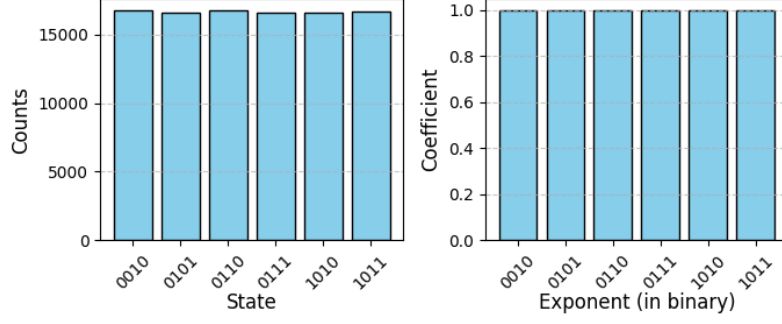


Fig. 5. The measurement counts (left panel) and the rounded coefficient p_i/p_{\min} (right panel) obtained from the output of QMbead for calculating 33×100 . The digits in the x-axis should be read from bottom left to top right. According to Eq. (11), the product is determined from the right panel as $1 \times 2^2 + 1 \times 2^5 + 1 \times 2^6 + 1 \times 2^7 + 1 \times 2^{10} + 1 \times 2^{11}$, which is equal to 3300.

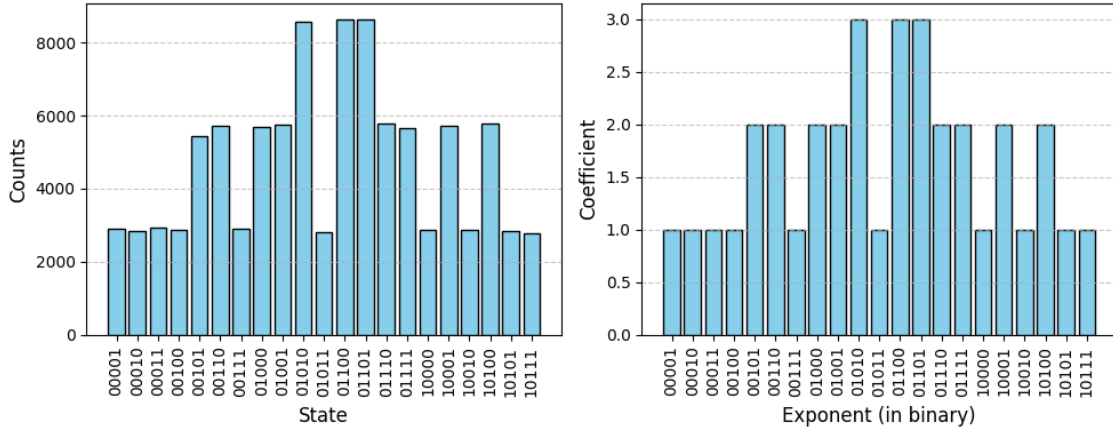


Fig. 6. The measurement counts (left panel) and the rounded coefficient p_i/p_{\min} (right panel) obtained from the output of QMbead for calculating 2345×5678 . The digits in the x-axis should be read from bottom to top. According to Eq. (11), the product is determined from the right panel as $2^1 + 2^2 + 2^3 + 2^4 + 2 \times 2^5 + 2 \times 2^6 + 2^7 + 2 \times 2^8 + 2 \times 2^9 + 3 \times 2^{10} + 2^{11} + 3 \times 2^{12} + 3 \times 2^{13} + 2 \times 2^{14} + 2 \times 2^{15} + 2^{16} + 2 \times 2^{17} + 2^{18} + 2 \times 2^{20} + 2^{21} + 2^{23}$, which is equal to 13314910.

V. Conclusion

This paper introduces the QMbead method designed for efficient multiplication of both integer and decimal numbers. QMbead requires a minimum of $2\lceil \log_2 n \rceil + 1$ qubits to accurately multiply two n -bit numbers and its circuit depth has a complexity of $O(\lceil \log_2 n \rceil^2)$. To achieve precise product calculations, the number of measurement shots must be sufficiently large, scaling linearly with the bit length of the product. In our implementation, two versions of QFT-based quantum adders were employed for QMbead. However, alternative types of quantum adders with lower circuit depth can be integrated into QMbead, further optimizing its efficiency. QMbead has demonstrated effectiveness in the multiplication of large integers (up to 273 bits in our numerical study) or decimal numbers with many bits, showcasing potential applications in large integer factorization challenges.

Acknowledgments

We acknowledge the support from the NSF ERI program, under award number 2138702. This work used the Delta system at the National Center for Supercomputing Applications through allocations CIS220136 and ELEC220008 from the Advanced Cyberinfrastructure Coordination Ecosystem: Services & Support

(ACCESS) program, which is supported by National Science Foundation grants #2138259, #2138286, #2138307, #2137603, and #2138296.

Appendix

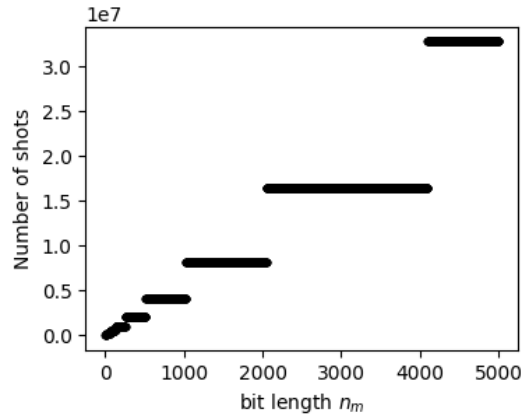


Fig. S1. The scatter plot showing the relationship between the number of shots needs and the bit length, n_m , of the larger multiplicand, i.e., a plot of the function $2000 \times 2^{1+\lceil \log_2 n_m \rceil}$.

Reference

- [1] P. W. Shor, “Algorithms for quantum computation: Discrete logarithms and factoring,” *Proceedings - Annual IEEE Symposium on Foundations of Computer Science, FOCS*, pp. 124–134, 1994, doi: 10.1109/SFCS.1994.365700.
- [2] P. W. Shor, “Polynomial-time algorithms for prime factorization and discrete logarithms on a quantum computer,” *SIAM J. Comput.*, vol. 26, no. 5, pp. 1484–1509, 1997, doi: 10.1137/s0097539795293172.
- [3] A. N. Nagamani, S. Ashwin, and V. K. Agrawal, “Design of optimized reversible binary adder/subtractor and BCD adder,” *Proceedings of 2014 International Conference on Contemporary Computing and Informatics, IC3I 2014*, pp. 774–779, Jan. 2014, doi: 10.1109/IC3I.2014.7019664.
- [4] T. G. Draper, S. A. Kutin, E. M. Rains, and K. M. Svore, “A logarithmic-depth quantum carry-lookahead adder,” *Quantum Inf Comput*, vol. 6, no. 4–5, pp. 351–369, Jun. 2004, doi: 10.26421/qic6.4-5-4.
- [5] V. Vedral, A. Barenco, and A. Ekert, “Quantum networks for elementary arithmetic operations,” *Phys Rev A (Coll Park)*, vol. 54, no. 1, p. 147, Jul. 1996, doi: 10.1103/PhysRevA.54.147.
- [6] P. Gossett, “Quantum Carry-Save Arithmetic,” Aug. 1998, Accessed: Sep. 09, 2023. [Online]. Available: <https://arxiv.org/abs/quant-ph/9808061v2>
- [7] S. A. Cuccaro, T. G. Draper, S. A. Kutin, and D. P. Moulton, “A new quantum ripple-carry addition circuit,” Oct. 2004, Accessed: Sep. 08, 2023. [Online]. Available: <https://arxiv.org/abs/quant-ph/0410184v1>
- [8] D. Beckman, A. N. Chari, S. Devabhaktuni, and J. Preskill, “Efficient networks for quantum factoring,” *Phys Rev A (Coll Park)*, vol. 54, no. 2, p. 1034, Aug. 1996, doi: 10.1103/PhysRevA.54.1034.
- [9] R. Rines and I. Chuang, “High Performance Quantum Modular Multipliers,” *ArXiv*, 2018.
- [10] L. Ruiz-Perez and J. C. Garcia-Escartin, “Quantum arithmetic with the Quantum Fourier Transform,” *Quantum Inf Process*, vol. 16, no. 6, Nov. 2014, doi: 10.1007/s11128-017-1603-1.
- [11] C. Gidney, “Asymptotically Efficient Quantum Karatsuba Multiplication,” Apr. 2019, Accessed: Sep. 09, 2023. [Online]. Available: <https://arxiv.org/abs/1904.07356v1>
- [12] H. M. H. Babu, “Cost-efficient design of a quantum multiplier–accumulator unit,” *Quantum Inf Process*, vol. 16, no. 1, pp. 1–38, Jan. 2017, doi: 10.1007/S11128-016-1455-0/METRICALS.

- [13] S. Kotiyal, H. Thapliyal, and N. Ranganathan, “Circuit for reversible quantum multiplier based on binary tree optimizing ancilla and garbage bits,” *Proceedings of the IEEE International Conference on VLSI Design*, pp. 545–550, 2014, doi: 10.1109/VLSID.2014.101.
- [14] J. J. Álvarez-Sánchez, J. V. Álvarez-Bravo, and L. M. Nieto, “A quantum architecture for multiplying signed integers,” *J Phys Conf Ser*, vol. 128, no. 1, p. 012013, Aug. 2008, doi: 10.1088/1742-6596/128/1/012013.
- [15] S. M. Cho, A. Kim, D. Choi, B. S. Choi, and S. H. Seo, “Quantum Modular Multiplication,” *IEEE Access*, vol. 8, pp. 213244–213252, 2020, doi: 10.1109/ACCESS.2020.3039167.
- [16] X. D. Zhang, X. M. Zhang, and Z. Y. Xue, “Quantum hyperparallel algorithm for matrix multiplication,” *Scientific Reports 2016 6:1*, vol. 6, no. 1, pp. 1–7, Apr. 2016, doi: 10.1038/srep24910.
- [17] H. Buhrman, B. Nl Robertšpalek, and R. Robertšpalek, “Quantum Verification of Matrix Products,” *Proceedings of the Annual ACM-SIAM Symposium on Discrete Algorithms*, pp. 880–889, Sep. 2004, doi: 10.1145/1109557.1109654.
- [18] R. Kothari and A. Nayak, “Quantum Algorithms for Matrix Multiplication and Product Verification,” *Encyclopedia of Algorithms*, pp. 1–6, 2015, doi: 10.1007/978-3-642-27848-8_303-2.
- [19] A. M. Childs, S.-H. Hung, and T. Li, “Quantum query complexity with matrix-vector products,” *Leibniz International Proceedings in Informatics, LIPIcs*, vol. 198, Feb. 2021, doi: 10.4230/LIPIcs.ICALP.2021.55.
- [20] C. Shao, “Quantum Algorithms to Matrix Multiplication,” Mar. 2018, Accessed: Sep. 08, 2023. [Online]. Available: <https://arxiv.org/abs/1803.01601v2>
- [21] A. Pavlidis and D. Gizopoulos, “Fast Quantum Modular Exponentiation Architecture for Shor’s Factorization Algorithm,” *Quantum Inf Comput*, vol. 14, no. 7–8, pp. 649–682, Jul. 2012, doi: 10.48550/arxiv.1207.0511.
- [22] N. Wiebe and M. Roetteler, “Quantum arithmetic and numerical analysis using Repeat-Until-Success circuits,” *Quantum Inf Comput*, vol. 16, no. 1–2, pp. 134–178, Jun. 2014, doi: 10.26421/qic16.1-2-9.
- [23] T. G. Draper, “Addition on a Quantum Computer,” Aug. 2000, Accessed: Aug. 11, 2023. [Online]. Available: <https://arxiv.org/abs/quant-ph/0008033v1>
- [24] V. Bergholm *et al.*, “PennyLane: Automatic differentiation of hybrid quantum-classical computations.” arXiv, 2018. doi: 10.48550/ARXIV.1811.04968.